First-Principles Investigation of Structural and Electronic Properties of the $B_xGa_{1-x}N$, $B_xAl_{1-x}N$, $Al_xGa_{1-x}N$ and $B_xAl_yGa_{1-x-y}N$ Compounds

L. Djoudi[a,b,*], A. Lachebi[a], B. Merabet[a] and H. Abid[a]

[a]Applied Materials Laboratory, Research Center, Sidi Bel Abbes University, 22000, Algeria

[b]University of Tissemsilt, Institute of Science and Technology, 38000, Algeria

(Received January 17, 2012; in final form August 4, 2012)

The structural and electronic properties of the $B_xGa_{1-x}N$, $B_xAl_{1-x}N$, $Al_xGa_{1-x}N$ and $B_xAl_yGa_{1-x-y}N$ compounds were studied using the full-potential linearized augmented plane wave method, within the generalized gradient approximation. We have compared the Al and B compositions dependence on the ground state properties: lattice parameters, bulk moduli and their pressure derivative, and band gap energies. The lattice parameters are found to change linearly for $Al_xGa_{1-x}N$, exhibit a downward bowing for both $B_xAl_{1-x}N$ and $B_xGa_{1-x}N$, and has a very small deviation when Al is added and a large deviation when B is incorporated for $B_xAl_yGa_{1-x-y}N$. The calculated band gap variation for the ternaries shows that the $B_xGa_{1-x}N$ has a phase transition from direct-gap to indirect-gap for high boron contents ($x > 0.75$). As for $B_xAl_{1-x}N$, a direct-gap is found in the boron content range $0.07 < x < 0.83$. For $Al_xGa_{1-x}N$ and $B_xAl_yGa_{1-x-y}N$ compounds, they have been found to be direct-gap materials. The results show that the $B_xGa_{1-x}N$, $B_xAl_{1-x}N$, $Al_xGa_{1-x}N$ and $B_xAl_yGa_{1-x-y}N$ materials may well be useful for optoelectronic applications.

PACS: 71.15.Mb, 71.20.−b, 71.20.Nr, 71.55.Eq

1. Introduction

Over the last few years, group III nitrides and their compounds have attracted a great deal of attention as being among the most important materials systems for optoelectronic and electronic applications [1]. Gallium nitride (GaN), aluminum nitride (AlN) and related materials are of considerable current interest because of their applications in light emitting devices operating in the visible and deep ultraviolet (UV) spectral regions [2–7]. Boron nitride (BN) is a very good choice for protective coatings due to its hardness, high melting point and large bulk modulus for the cubic variety [8]. BN, on the other hand, has features of high thermal conductivity suitable for applications in electronic devices [9].

Actually, high sensitivity avalanche photodiode detectors and compact lasers operating in UV range are needed for different applications such as biomedical, purification, convert communication and real-time detection of airborne pathogens [10]. Among the most promising candidate for lasers operating in the deep-UV spectral region is the BAlGaN system [11], derived from GaN, AlN and BN. It can be lattice matched to 6H-SiC and AlN substrates [12], and exhibit band-gap energies ranging from 3.6 eV to 6.2 eV and from 3.8 eV to 6.2 eV when lattice matched to AlN and 6H-SiC substrates, respectively, and corresponding wavelengths in the range 344 nm to 200 nm [13].

Takano et al. [11] studied the crystal growth of the BAlGaN system using the low-pressure metalorganic vapor phase epitaxy (LP-MOVPE) to grow (BAlGaN) and (BAlGaN/AlN), using triethylboron (TEB), trimethylaluminum (TMAl), trimethylgallium (TMGa) and ammonia (NH_3) as source materials respectively for B, Al, Ga and N atoms, and the Auger electron spectroscopy (AES) and X-ray diffraction (XRD) to control the B, Al, Ga and N compositions in $B_xAl_yGa_{1-x-y}N$ layers.

In this present work, we have studied the structural and electronic properties of the $B_xGa_{1-x}N$, $B_xAl_{1-x}N$, $Al_xGa_{1-x}N$ ternaries and $B_xAl_yGa_{1-x-y}N$ quaternary systems over the entire compositions x and y by performing *ab initio* calculations, based on the full-potential linearized augmented plane wave (FP-LAPW) method within the density functional theory (DFT) as implemented in the WIEN2K code [14].

The plan of the present paper is as follows: after a description of the method as well as some details of the calculations in Sect. 2, the lattice parameters and band-gap energies of BN, AlN, GaN, $B_xGa_{1-x}N$, $B_xAl_{1-x}N$, $Al_xGa_{1-x}N$ and $B_xAl_yGa_{1-x-y}N$ compounds are presented and discussed in Sect. 3. Finally, a brief conclusion of the present study is given in Sect. 4.

2. Calculation method

In this study, the structural properties and band gap energies of $B_xGa_{1-x}N$, $B_xAl_{1-x}N$, $Al_xGa_{1-x}N$ and $B_xAl_yGa_{1-x-y}N$ solid solutions are investigated using the FP-LAPW simulation program approach based on the density functional theory, where we have used as approximation for the calculation of exchange-correlation energy functional: the well-known generalized gradient approximation (GGA) due to Wu and Cohen [15].

To model $A_xB_{1-x}N$ compound, we have applied a 16-atom $A_nB_{8-n}N_8$ supercell, which corresponds to a $2\times2\times2$ supercell that is twice the size of a primitive unit cell in base plane direction. As for $B_xAl_yGa_{1-x-y}N$, we

* corresponding author; e-mail: djoudilakhdar@yahoo.fr

also have applied a 16-atom $B_aAl_bGa_{8-a-b}N_8$ supercell, with $a+b \leq 8$.

In the FP-LAPW calculations, each unit cell is partitioned into non-overlapping muffin-tin spheres around the atomic sites. Basis functions are expanded in combinations of spherical harmonic functions inside the non-overlapping spheres. In the interstitial region, a plane wave basis is used and expansion is limited with a cut-off parameter, $R_{\mathrm{MT}}\, K_{\mathrm{MAX}} = 7$ for all the compounds. R_{MT} is the minimum radius (MF) of the sphere in the unit cell; K_{MAX} is the magnitude of the largest K vector used in the plane wave expansion. The MT radii are adopted to be 1.67, 1.74, and 1.67 bohr for B, Ga, and N atoms; 1.62, 1.68, and 1.62 bohr for B, Al, and N atoms; 1.76, 1.84, 1.62 bohr for Al, Ga, and N atoms; and 1.63, 1.67, 1.71, and 1.65 bohr for B, Al, Ga, and N atoms for $B_xGa_{1-x}N$, $B_xAl_{1-x}N$, $Al_xGa_{1-x}N$ and $B_xAl_yGa_{1-x-y}N$ solid solutions, respectively.

The semi-relativistic approximation without spin–orbit effects was employed in our calculations, where the core levels are treated fully relativistically [16]. We have distinguished the Ga ($1s^2 2s^2 2p^6 3s^2 3p^6$), N ($1s^2$), B ($1s^2$) and Al ($1s^2 2s^2 2p^6$) inner-shell electrons from the valence electrons of Ga ($3d^{10} 4s^2 4p^1$), N ($2s^2 2p^3$), B ($2s^2 2p^1$) and Al ($3s^2 3p^1$) shells, by choosing a cut-off energy of -6.0 Ry for binaries and -8.0 Ry for ternaries and quaternaries. The expansion of spherical harmonic functions inside the MT spheres is truncated at $l_{\max} = 10$. The cut-off for the Fourier expansion of the charge density is fixed to be $G_{\mathrm{MAX}} = 12$ for all compounds and compounds. For the irreducible wedge of the Brillouin zone, meshes of 56 and 14 special k-points were used for binaries and all compounds, respectively.

3. Results and discussions

3.1. Structural parameters

The $B_xAl_yGa_{1-x-y}N$ quaternary system is bounded by three ternary systems: $B_xGa_{1-x}N$, $B_xAl_{1-x}N$, and $Al_xGa_{1-x}N$. These ternaries, in their turn, are made up of three binaries BN, AlN, and GaN. The ground-state structural parameters have been obtained by minimizing the total energy with respect to the volume, by fitting this total energy versus the volume data on the non-linear Murnaghan equation of state [17]. Hence, first we computed the lattice parameter of the three binaries in their cubic structure with the space group F-43m (no. 216). Then, we studied the ternaries with the selected x-compositions: 0.25, 0.5, and 0.75. For $x = 0.25$ and 0.75, the related space group is P-43m (no. 215); however, for $x = 0.50$ the crystal structure belongs to the P-4m2 (no. 115) space group, which is a tetragonal structure.

In Table I, we summarize the calculated lattice constants and the bulk module and its pressure derivative of binaries and ternaries together with the available experimental and theoretical data. As can be seen, the obtained lattice constants for binaries are in reasonable agreement with the experimental data [18, 19]. It is found out that the calculated bulk modulus and its pressure derivative for BN is 3.5% and 0.49% smaller, respectively, than the experimental value [20].

As for AlN, the calculated bulk modulus is 5.26% greater than the experimental value [21]. The lattice parameter of ternaries has been found to be deviated from Vegard's law [22] with the bowing parameters: -0.42 ± 0.041 Å, -0.306 ± 0.021 Å, and 0.017 ± 0.001 Å for $B_xGa_{1-x}N$, $B_xAl_{1-x}N$, and $Al_xGa_{1-x}N$, respectively. It is found out that the calculated bulk moduli for the $B_xGa_{1-x}N$ and $B_xAl_{1-x}N$ compounds increase non-linearly with the boron composition increasing as well as for $Al_xGa_{1-x}N$ with the aluminum composition increasing. A non-linear variation of the derivative of the bulk moduli for the ternaries has been also observed. To estimate the $B_xAl_yGa_{1-x-y}N$ lattice parameters dependence on B and Al concentrations, we have performed a list of calculations for $B_xAl_yGa_{1-x-y}N$ for different B and Al compositions.

In Table II, we summarize the calculated lattice constants, the bulk moduli and their pressure derivatives and the structure's nature of $B_xAl_yGa_{1-x-y}N$. Obviously, the change of phase corresponding to different values of the compositional parameter x and y for the $B_xAl_yGa_{1-x-y}N$ compound (216/F-43m/cubic, 119/I-4m2/tetragonal and 22/$F$222/orthorhombic) has a predictive character, which one would expect from the DFT calculations, and is subject to the experimental verification.

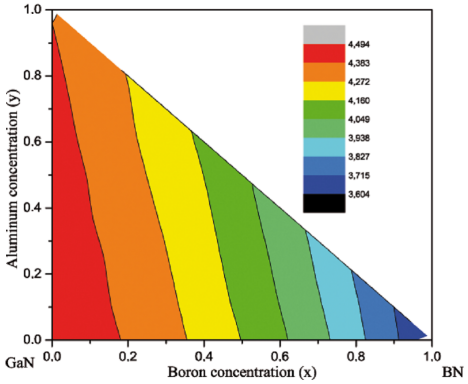

Fig. 1. Formation lattice constant contour at different concentrations (x, y) of $B_xAl_yGa_{1-x-y}N$ compound.

According to the results plotted in Fig. 1, the lattice constant of $B_xAl_yGa_{1-x-y}N$ depending on B and Al-concentrations can be fitted as follows:

$$a(x,y) = 4.494 - 0.536x - 0.387x^2 - 0.124y - 0.0002y^2. \quad (1)$$

These results indicate that the $B_xAl_yGa_{1-x-y}N$ lattice constant has a very small deviation and decreases when Al is added, and has a large deviation and decreases when B is incorporated. These results might be due to the size and electronegativity mismatch between B and Al atoms atoms ($\chi_{\mathrm{B}} = 2.04$ and $\chi_{\mathrm{Al}} = 1.61$). This equation allows us to calculate the lattice parameter for $B_xAl_yGa_{1-x-y}N$

with any boron and aluminum concentrations. It is very clear from Table II that the calculated bulk modulus (and its pressure derivative) for $B_xAl_yGa_{1-x-y}N$ varies non-linearly with increasing either boron or aluminum compositions.

TABLE I

Calculated lattice parameter (a) and bulk module (B_0) and its pressure derivative (B'_0) for the GaN, AlN, BN, $B_xGa_{1-x}N$, $B_xAl_{1-x}N$ and $Al_xGa_{1-x}N$ compounds. Available experimental and theoretical data are also given for comparison. a [Å], B_0 [GPa] and B'_0 [GPa].

	Present work			Experimental works			Other theoretical works		
	a	B_0	B'_0	a	B_0	B'_0	a	B_0	B'_0
BN	3.605	386	4.08	3.615[a], 3.59[b]	400[b]	4.1[b]	3.63[e], 3.58[f]	371[e], 401.7[f]	3.7[e], 3.66[f]
AlN	4.377	201	3.66	4.37[a]	–	–	4.346[g]	206[i], 212[g]	3.97[i], 3.77[g]
GaN	4.494	200	4.75	4.49[a], 4.50[b], 4.53[c]	190[d]	–	4.46[e], 4.51[h]	202[e], 191[h]	4.43[e], 4.14[h]
$B_{0.25}Ga_{0.75}N$	4.341	220	4.23	–	–	–	4.38[e], 4.31[j]	198[e], 226[j]	4.19[e], 4.1[j]
$B_{0.50}Ga_{0.50}N$	4.158	229	4.58	–	–	–	4.19[e], 4.13[j]	235[e], 261[j]	4.77[e], 3.88[j]
$B_{0.75}Ga_{0.25}N$	3.918	299	4.06	–	–	–	3.9[e], 3.86[j]	302[e], 287[j]	3.15[e], 3.8[j]
$B_{0.25}Al_{0.75}N$	4.236	219	4.52	–	–	–	4.18[k]	214[l]225[m]	–
$B_{0.50}Al_{0.50}N$	4.069	238	4.34	–	–	–	3.97[k]	245[l]257[m]	–
$B_{0.75}Al_{0.25}N$	3.861	298	4.12	–	–	–	3.75[k]	296[l]312[m]	–
$Al_{0.25}Ga_{0.75}N$	4.468	194	4.88	–	–	–	4.39[n]	203[n]	4.39[n]
$Al_{0.50}Ga_{0.50}N$	4.440	196	4.81	–	–	–	4.41[n]	205[n]	4.46[n]
$Al_{0.75}Ga_{0.25}N$	4.409	196	4.50	–	–	–	4.37[n]	207[n]	4.53[n]

[a] Ref. [18], [b] Ref. [20], [c] Ref. [19], [d] Ref. [21], [e] Ref. [24], [f] Ref. [25], [g] Ref. [26], [h] Ref. [27], [i] Ref. [28], [j] Ref. [29], [k] Ref. [30], [l] Ref. [31], [m] Ref. [32], [n] Ref. [33]

TABLE III

The direct-gap $E_{g(\Gamma-\Gamma)}$ and indirect-gap $E_{g(\Gamma-X)}$ for the BN, AlN, GaN, $B_xGa_{1-x}N$, $B_xAl_{1-x}N$, and $Al_xGa_{1-x}N$ compounds. Available experimental and theoretical data are also given for comparison.

	Gap [eV]	Present work	Other theoretical	Experimental
		GGA(WC)	works	works
BN	$E_{g(\Gamma-\Gamma)}$	8.59	7.78[e], 8.79°, 8.89[j]	–
	$E_{g(\Gamma-X)}$	4.22	4.35[e], 4.47°	–
AlN	$E_{g(\Gamma-\Gamma)}$	4.10	4.13[j]	–
	$E_{g(\Gamma-X)}$	3.20	–	–
GaN	$E_{g(\Gamma-\Gamma)}$	1.64	1.52[e], 2.1[p]	3.2[q]
	$E_{g(\Gamma-X)}$	3.19	3.22[e]	–
$B_{0.25}Ga_{0.75}N$	$E_{g(\Gamma-\Gamma)}$	2.78	2.73[e], 2.95[j]	–
	$E_{g(\Gamma-X)}$	4.36	3.48[e], 4.45[j]	–
$B_{0.50}Ga_{0.50}N$	$E_{g(\Gamma-\Gamma)}$	3.22	3.26[e], 3.4[j]	–
	$E_{g(\Gamma-X)}$	5.28	4.03[e], 5.36[j]	–
$B_{0.75}Ga_{0.25}N$	$E_{g(\Gamma-\Gamma)}$	3.65	3.67[e], 3.9[j]	–
	$E_{g(\Gamma-X)}$	5.15	4.27[e], 6.3[h]	–
$B_{0.25}Al_{0.75}N$	$E_{g(\Gamma-\Gamma)}$	3.47	3.7[l], 3.45[r]	–
	$E_{g(\Gamma-X)}$	5.50	–	–
$B_{0.50}Al_{0.50}N$	$E_{g(\Gamma-\Gamma)}$	3.62	4.4[l], 3.64[r]	–
	$E_{g(\Gamma-X)}$	6.28	–	–
$B_{0.75}Al_{0.25}N$	$E_{g(\Gamma-\Gamma)}$	4.03	4.9[l], 4.05[r]	–
	$E_{g(\Gamma-X)}$	6.07	–	–
$Al_{0.25}Ga_{0.75}N$	$E_{g(\Gamma-\Gamma)}$	2.22	2.221[s]	–
	$E_{g(\Gamma-X)}$	4.82	4.80[n]	–
$Al_{0.50}Ga_{0.50}N$	$E_{g(\Gamma-\Gamma)}$	2.77	2.781[s]	–
	$E_{g(\Gamma-X)}$	5.14	4.75[n]	–
$Al_{0.75}Ga_{0.25}N$	$E_{g(\Gamma-\Gamma)}$	3.24	3.503[s]	–
	$E_{g(\Gamma-X)}$	5.53	4.65[n]	–

[o] Ref. [34], [p] Ref. [35], [q] Ref. [36], [r] Ref. [37], [s] Ref. [38]

TABLE II

Calculated lattice parameter (a), bulk module (B_0) and its pressure derivative (B_0') and structure for the $B_xAl_yGa_{1-x-y}N$ compounds for different B and Al compositions.

(x, y)	Structure	a [Å]	B_0 [GPa]	B_0' [GPa]
(0.125, 0.125)	216/F-43m/cubic	4.40	212	4.87
(0.125, 0.25)	119/I-4m2/tetragonal	4.39	220	4.12
(0.125, 0.375)	119/I-4m2/tetragonal	4.37	214	4.07
(0.125, 0.5)	119/I-4m2/tetragonal	4.36	203	4.71
(0.125, 0.625)	119/I-4m2/tetragonal	4.34	209	4.01
(0.125, 0.75)	216/F-43m/cubic	4.33	205	4.55
(0.25, 0.125)	119/I-4m2/tetragonal	4.32	223	3.88
(0.25, 0.25)	111/P-42m/tetragonal	4.31	222	4.15
(0.25, 0.375)	22/$F$222/orthorhombic	4.29	202	4.54
(0.25, 0.5)	111/P-42m/tetragonal	4.27	214	4.60
(0.25, 0.625)	119/I-4m2/tetragonal	4.25	219	4.65
(0.375, 0.125)	119/I-4m2/tetragonal	4.24	221	4.16
(0.375, 0.25)	119/I-4m2/tetragonal	4.22	227	4.11
(0.375, 0.375)	22/$F$222/orthorhombic	4.20	241	3.57
(0.375, 0.5)	119/I-4m2/tetragonal	4.18	224	4.44
(0.5, 0.125)	119/I-4m2/tetragonal	4.13	267	3.25
(0.5, 0.25)	111/P-42m/tetragonal	4.11	243	4.43
(0.5, 0.375)	119/I-4m2/tetragonal	4.09	251	3.86
(0.625, 0.125)	119/I-4m2/tetragonal	4.02	277	3.78
(0.625, 0.25)	119/I-4m2/tetragonal	4.00	256	4.49
(0.75, 0.125)	216/F-43m/cubic	3.89	302	3.86

3.2. Band gap energies

Knowing the energy band structures in semiconductors provides a valuable information as regards their potential utility in the fabrication of electronic and optoelectronic devices. As group III nitrides and their compounds are promising materials for their application in electronic and optoelectronic devices, the accurate knowledge of the band structures of the $B_xGa_{1-x}N$, $B_xAl_{1-x}N$, $Al_xGa_{1-x}N$ and $B_xAl_yGa_{1-x-y}N$ compounds becomes essential.

We have used the FP-LAPW method to calculate mainly the band-gap energies of BN, GaN, AlN, $B_xGa_{1-x}N$, $B_xAl_{1-x}N$, $Al_xGa_{1-x}N$ and $B_xAl_yGa_{1-x-y}N$ at the equilibrium calculated lattice constants.

The obtained Γ and X-band-gaps of semiconductor (SC) are listed in Table III and compared with the available experimental and theoretical data. The results show that GaN has a direct-gap with the minimum of conduction band at the Γ point; BN and AlN have an indirect--gap with the minimum energy gap at the X point. It is clearly seen that the band-gaps of SC are, on the whole, underestimated in comparison with the experimental results, and are in good agreement with the theoretical data listed in Table III. The large difference in the calculated values of the band gaps as compared to the experimental values can be explained by the fact that, in the electronic band structure calculations within DFT, the GGA underestimates the energy band gap in semiconductors, and it can be demonstrated that within these approximations, the self-interaction error and the absence of derivative discontinuity in the exchange-correlation potential cause a significant underestimation (up to 50%) of the band gap [23].

The band-gap energy of an $A_xB_{1-x}C$ compound can be depicted as a function of the A composition x, and can be approximated using the following Eq. (2):

$$E_g(x) = xE_{gAC} + (1-x)E_{gBC} - x(1-x)b, \qquad (2)$$

where $E_g(x)$ is the band-gap energy of the $A_xB_{1-x}C$ solution; E_{gAC} and E_{gBC} are the band-gap energies of the binary compounds AC and BC, respectively, and the quadratic term b is the bowing parameter of $A_xB_{1-x}C$.

After the good fitting, the band-gap energies of the $B_xGa_{1-x}N$, $B_xAl_{1-x}N$ and $Al_xGa_{1-x}N$ obtained with the equilibrium lattice are plotted in Fig. 2, Fig. 3 and Fig. 4, respectively.

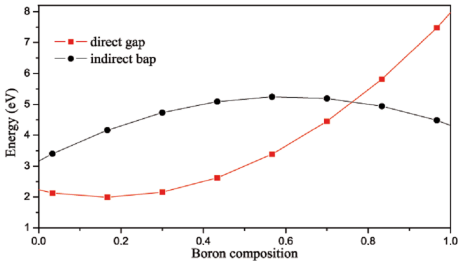

Fig. 2. The energy band-gaps of $B_xGa_{1-x}N$ as a function of boron composition.

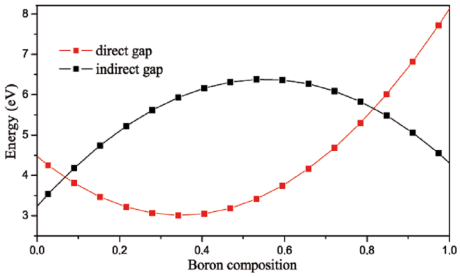

Fig. 3. The energy band-gaps of $B_xAl_{1-x}N$ as a function of boron composition.

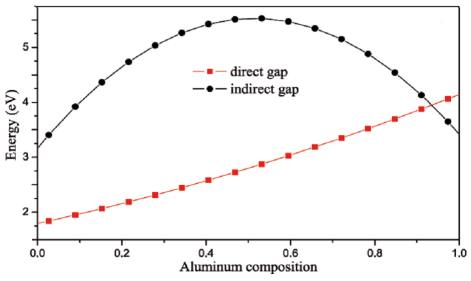

Fig. 4. The energy band-gaps of $Al_xGa_{1-x}N$ as a function of aluminum composition.

The $B_xGa_{1-x}N$ has a phase transition from direct to indirect-gap for high boron contents ($x > 0.75$). For

$B_xAl_{1-x}N$, a direct-gap is found for $0.07 < x < 0.83$. As for $Al_xGa_{1-x}N$, its gap has been found entirely direct.

The calculated band structures of $B_xAl_yGa_{1-x-y}N$ compound for different x and y values, using the GGA (WC) scheme, have been displayed in Fig. 5, where we have taken as an example four pairs of (x, y) concentrations, (0.125, 0.5), (0.25, 0.375), (0.375, 0.125), and (0.75, 0.125). One can clearly see the direct nature of the band gap of this compound.

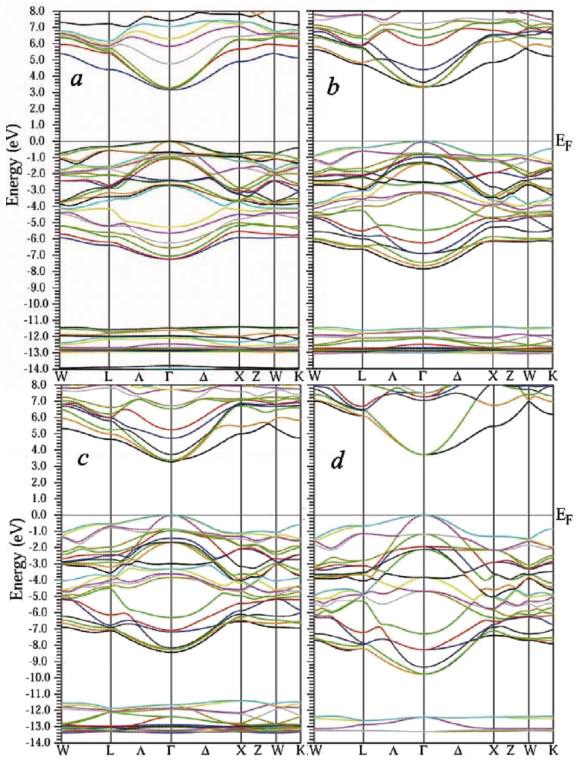

Fig. 5. The band structure of $B_xAl_yGa_{1-x-y}N$: (a) $B_{0.125}Al_{0.50}Ga_{0.375}N$, (b) $B_{0.25}Al_{0.375}Ga_{0.375}N$, (c) $B_{0.375}Al_{0.125}Ga_{0.5}N$, (d) $B_{0.75}Al_{0.125}Ga_{0.125}N$.

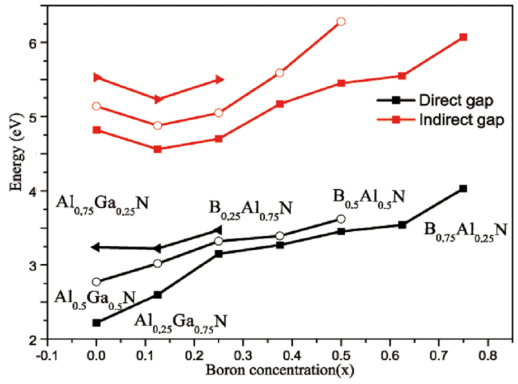

Fig. 6. The energy band-gaps of $B_xAl_yGa_{1-x-y}N$ with the compositional parameter y having the 0.25, 0.5 and 0.75 and $(0 \le x \le 1)$ where $(x + y \le 1)$.

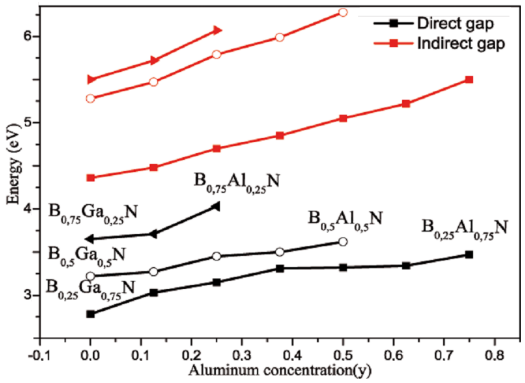

Fig. 7. The energy band-gaps of $B_xAl_yGa_{1-x-y}N$ with the compositional parameter x having the 0.25, 0.5 and 0.75 and $(0 \le y \le 1)$, where $(x + y \le 1)$.

We have plotted the energy band-gaps for $B_xAl_yGa_{1-x-y}N$ with the compositional parameter y taken to be 0.25, 0.5 and 0.75 as shown in Fig. 6 and with the compositional parameter x having the 0.25, 0.5 and 0.75 as shown in Fig. 7. Both figures show that the quaternary have a direct gap and the boron induced leads to an increase of the gap over a large range of 81.53%, and the aluminum induced leads to an increase of the gap over a range of 24.82%, the curves of two figures obey the following variations:

direct gap

$$E_{\Gamma-\Gamma}(x, y) = 3.285 + 0.621x - 1.8x^2 + 0.969y + 1.885y^2, \quad (3)$$

indirect gap

$$E_{\Gamma-X}(x, y) = 4.097 + 0.533x - 0.647x^2 + 2.735y + 0.372y^2. \quad (4)$$

The two equations allow us to calculate the direct and indirect gap for any concentration x (boron) and y (aluminum) of the quaternary $B_xAl_yGa_{1-x-y}N$, with $x + y \le 1$. It is clearly seen that the direct and indirect band-gaps increase non-linearly with the increase of the concentrations x and y, and this quaternary is a direct-gap material over the whole range of x and y.

4. Conclusion

The FP-LAPW method, within the GGA is utilized to investigate the structural properties and band gap energies of BN, GaN, AlN, $B_xGa_{1-x}N$, $B_xAl_{1-x}N$, $Al_xGa_{1-x}N$ and $B_xAl_yGa_{1-x-y}N$ compounds. From the calculated results, it is found that the lattice constant of each binary is in reasonable agreement with the experimental values. The bowing parameters of the lattice constant for $B_xGa_{1-x}N$, $B_xAl_{1-x}N$ and $Al_xGa_{1-x}N$ are -0.42 ± 0.041 Å, -0.306 ± 0.021 Å and 0.017 ± 0.001 Å, respectively. For $x > 0.75$, a phase transition from direct to indirect gap for $B_xGa_{1-x}N$ compound occurs at the band gap energy of 5.1 eV. For the $B_xAl_{1-x}N$ compound, the direct-gap is found in the range $0.07 < x < 0.83$ of

boron contents, while $Al_xGa_{1-x}N$ is a direct-gap material over the entire range of the aluminum content (x).

The calculated structural and electronic properties of the $B_xAl_yGa_{1-x-y}N$ compound for different boron and aluminum compositions (x, y) show a linear behavior of the lattice constant and a non-linear behavior of the direct and indirect band-gaps. The incorporation of boron decreases the lattice parameter of the quaternary by 15.72% and increases the energy gap by 81.53%, while the incorporation of aluminum reduces the lattice parameter by 2.45% and increases the energy gap by 24.82%, which gives a great importance for the boron incorporation.

Finally, it has been found that this compound is a direct gap material. This essential characteristic indicates that those materials ($B_xGa_{1-x}N$, $B_xAl_{1-x}N$, $Al_xGa_{1-x}N$, and $B_xAl_yGa_{1-x-y}N$) can be useful for optoelectronic applications. The calculated band-gap energy of BAlGaN is in the range of 3.121 eV to 5.122 eV, corresponding to the wavelength range of 397 nm to 242 nm. Therefore, the BAlGaN system is a promising material for use in semiconductor lasers that operate in the ultraviolet (UV) spectral region.

References

[1] Shuji Nakamura, *J. Vac. Sci. Technol. A* **13**, 705 (1995).

[2] S. Strite, H. Morkoç, *J. Vac. Sci. Technol. B* **10**, 1237 (1992).

[3] C.G. Van de Walle, *Physica B* 185, ix-x (1993).

[4] H. Morkoç, S. Strite, G.B. Gao, M.E. Lin, B. Sverdlov, M. Burns, *J. Appl. Phys.* **76**, 1363 (1994).

[5] F.A. Ponce, D.P. Bour, *Nature* **386**, 351 (1997).

[6] S. Nakamura, *Solid State Commun.* **102**, 237 (1997).

[7] J. Chen, Z.H. Levine, J.W. Wilkins, *Appl. Phys. Lett.* **66**, 1129 (1995).

[8] H. Wang, H. Xu, X. Wang, C. Jiang, *Phys. Lett. A* **373**, 2082 (2009).

[9] T. Takayama, M. Yuri, K. Itoh, T. Baba, J.S. Harris Jr, *J. Cryst. Growth.* **222**, 29 (2001).

[10] A. Ougazzaden, S. Gautier, C. Sartel, N. Maloufi, J. Martin, F. Jomard, *J. Cryst. Growth.* **298**, 316 (2007).

[11] T. Takano, M. Kurimoto, J. Yamamoto, H. Kawanishi, *J. Cryst. Growth.* **237-239**, 972 (2002).

[12] M. Haruyama, T. Shirai, H. Kawanishi, Y. Suematsu, in: *Proc. Int. Symp. on Blue Laser and Light Emitting Diodes*, Chiba University, Chiba 1996, p. 106.

[13] M. Tsubamoto, T. Honda, J. Yamamoto, M. Kurimoto, M. Shibata, M. Haruyama, H. Kawanishi, in: *Proc. Second Int. Conf. on Nitride Semiconductors*, Tokushima 1997, p. 250.

[14] P. Blaha, K. Schwarz, G.K.H. Madsen, D. Kvasnicka, J. Luitz, *WIEN2K, An Augmented Plane Wave+Local Orbitals Program for Calculating Crystal Properties*, Karlheinz Schwarz, Techn. Universität, Wien, Austria, 3-9501031-1-2, 2001.

[15] Z. Wu, R.E. Cohen, *Phys. Rev. B* **73**, 235116 (2006).

[16] D.D. Koelling, B.N. Harmon, *J. Phys. C* **10**, 3107 (1977).

[17] F.D. Murnaghan, *Proc. Natl. Acad. Sci. USA* **30**, 244 (1944).

[18] V.L. Solozhenho, in: *Properties of Group III Nitrides*, Electronics Materials Information Service (EMIS) Data Reviews Series, Ed. J.H. Edgar, Institution of Electrical Engineers, London 1994, p. 10.

[19] D. Vogel, P. Kruger, J. Pollmann, *Phys. Rev. B* **55**, 12836 (1997).

[20] A. Trampert, O. Brandt, K.H. Ploog, in: *Crystal Structure of Group III Nitrides Semiconductors and Semimetals*, Eds. J.I. Pankove, T.D. Moustakas, Academic Press, San Diego 1998.

[21] M.E. Sherwin, T.J. Drummond, *J. Appl. Phys.* **69**, 8423 (1987).

[22] L. Vegard, *Z. Phys.* **5**, 17 (1921).

[23] A. Shaukat, Y. Saeed, S. Nazir, M. Tanveer, *Physica B* **404**, 3964 (2009).

[24] R. Riane, Z. Boussahl, A. Zaoui, L. Hammerelaine, S.F. Matar, *Solid State Sci.* **11**, 200 (2009).

[25] K. Kim, W.R.L. Lambrecht, B. Segall, *Phys. Rev. B* **53**, 16310 (1996).

[26] B. Daoudi, M. Sehil, A. Boukraa, H. Abid, *Int. J. Nanoelectron. Mater.* **1**, 65 (2008).

[27] C. Stampfl, C.G. Van de Walle, *Phys. Rev. B* **59**, 5521 (1999).

[28] L.E. Ramos, J. Furthmuller, F. Bechstedt, L.M.R. Scolfaro, J.R. Leite, *J. Phys., Condens. Matter.* **14**, 2577 (2002).

[29] A. Lachebi, H. Abid, *Turk. J. Phys.* **32**, 157 (2008).

[30] L.K. Teles, L.M.R. Scolfaro, J.R. Leite, J. Furthmuller, F. Bechstedt, *Appl. Phys. Lett.* **80**, 1177 (2002).

[31] V.V. Ilyasov, T.P. Zhdanova, I.Ya. Nikiforov, *Phys. Solid State* **47**, 1618 (2005).

[32] Jin-Cheng Zheng, Hui-Qiong Wang, C.H.A. Huan, A.T.S. Wee, *J. Phys., Condens. Matter* **13**, 5295 (2001).

[33] B.-T. Liou, *Appl. Phys. A* **86**, 539 (2007).

[34] A. Zaoui, F. El Haj Hassan, *J. Phys., Condens. Matter* **13**, 253 (2001).

[35] L.E. Ramos, L.K. Teles, L.M.R. Scolfaro, J.L.P. Castineira, A.L. Rosa, J.R. Leite, *Phys. Rev. B* **63**, 165210 (2001).

[36] T. Lei, T.D. Moustakas, R.J. Graham, Y. He, S.J. Berkowitz, *J. Appl. Phys.* **71**, 4933 (1992).

[37] J.-C. Zheng, H.-Q. Wang, C.H.A. Huan, A.T.S. Wee, *J. Phys., Condens. Matter* **13**, 5295 (2001).

[38] D. Li, X. Zhang, Z. Zhu, H. Zhang, *Solid State Sci.* **13**, 1731 (2011).